J. Biochem. 125, 58-63 (1999)

Hydrophobic Interactions of Val75 Are Critical for Oligomeric Thermostability of Inorganic Pyrophosphatase from *Bacillus stearothermophilus*

Hiroshi Shinoda, Manabu Hattori, Atsushi Shimizu, Tatsuya Samejima,[1] and Takanori Satoh

Department of Chemistry, College of Science and Engineering, Aoyama Gakuin University, Chitosedai, Setagaya-ku, Tokyo 157-8572

Received July 14, 1998; accepted September 28, 1998

To determine the role of Val75 in the oligomeric structure of trimeric inorganic pyrophosphatase (PPase) [EC 3.6.1.1] from *Bacillus stearothermophilus* (*Bst.*), we used site-directed mutagenesis to prepare variants in which Val75 was replaced by Ala, Phe, Leu, Ile, Lys, Gln, and Asp. As a result, the variants in which valine is replaced by hydrophobic residues such as Ala, Phe, Leu, and Ile (V75A, F, L, and I) show almost the same level of enzyme activity and thermostability as the wild type enzyme, whereas variants with hydrophilic residue replacements such as Lys, Gln, and Asp (V75K, Q, and D) showed gross reductions in enzyme activity and thermostability. The dissociation of V75K and V75D from trimer to monomers occurred rapidly as the temperature rose, while V75F, V75L, and V75I dissociated more slowly than the wild type. There was no particular effect of heat treatment on the dissociation of V75A or V75Q, but these variants were slightly dissociated even in the native state. Thus, we conclude that Val75 may locate at the interface between the monomers and its hydrophobic interactions with its surroundings may play a key role in the thermostability and oligomeric subunit interactions of the enzyme.

Key words: *Bacillus stearothermophilus*, hydrophobic interaction, inorganic pyrophosphatase, site-directed mutagenesis, thermostability.

Inorganic pyrophosphatase (PPase, EC 3.6.1.1) catalyzes the hydrolysis of inorganic pyrophosphate, which is a product of many important reactions in organs and cells (*1*). Divalent metal ions are essential for the expression of PPase activity; in particular, magnesium ions induce the highest activity (*2*).

PPases are mainly classified into two groups, eucaryotic and procaryotic types. The best studied eucaryotic PPase is *Saccharomyces cerevisiae* PPase (Y-PPase). Site-directed studies of Y-PPase have indicated the roles of many residues in the active site (*3*), for which the three-dimensional structure was also determined at 2.2 and 2.0 Å resolution (*4*). The best studied procaryotic PPase is *Escherichia coli* PPase, which has been the target of many site-directed mutagenesis studies. The three-dimensional structure of *E. coli* PPase has identified the residues in the active center (*5, 6*). Substitution of His residues located at the interface between the trimers of *E. coli* PPase by site-directed mutagenesis produces a dissociation of the hexameric subunits into trimers (*7*). The three-dimensional structure of *Thermus thermophilus* (*Tth.*) PPase, a procaryotic type, was also determined by X-ray crystallography at 2.0 Å resolution (*8*). The characteristics of each monomer and the amino acid sequences in the vicinity of active site of these enzymes are very similar, and 17 putative active site residues are conserved (*9*). It has been reported that *E. coli* and *Tth.* PPases exist as hexamers, and their characterization, such as interactions between monomers or trimers, have been investigated in detail. It was determined that *Tth.* PPase is more thermostable than *E. coli* PPase because the oligomeric interactions contribute to thermostability (*10*).

A moderate thermophilic bacterium, *Bacillus stearothermophilus* (*Bst.*) has its optimal growth temperature at 65°C, and *Bst.* PPase shows higher thermostability in both its catalytic activity and conformation as compared with the PPase from *E. coli* (*2, 11*). Furthermore, the semi-synthetic *Bst.* PPase gene is effectively expressed in *E. coli* cells (*11*). Recently, PPase from the thermophilic bacterium PS-3 was cloned and expressed, and the amino acid sequence was found to be very similar to that of *Bst.* PPase (*12*). As for *Bst.* PPase, the three-dimensional structure has not yet been determined, but the amino acid sequence is similar to those of *E. coli* and *Tth.* PPases and the putative active site residues are predicted by its homology (*11*). Some characteristics of *Bst.* PPase such as the oligomeric structure and kinetics, have been reported (*13, 14*), however, the residues that contribute to the subunit interactions have not yet been identified. *Bst.* PPase exists as a trimer, so it is thought that the monomer-monomer

[1] To whom correspondence should be addressed. Tel: +81-3-5384-1111 (Ext. 3204), Fax: +81-3-5384-6200, E-mail: samejima@candy.chem.aoyama.ac.jp

Abbreviations: PPase, inorganic pyrophosphatase; *Bst.*, *Bacillus stearothermophilus*; *Tth.*, *Thermus thermophilus*; Y, *Saccharomyces cerevisiae*.

TABLE I. **The residues located in the intratrimer regions of *E. coli* and *Tth.* PPases (*10*).**

E. coli PPase	*Tth.* PPase	*Bst.* PPase[a]
Residues		Predicted residues
Ser1		
Leu2		
	Pro7	
Asp26		Ser17
Pro27		Glu18
Ile28	Asn28	Asn19
Tyr30	**Tyr30**	**Tyr21**
Ser36	Leu36	Arg27
Ala38		Ile29
Leu39	*Ile39*	*Phe30*
Phe40	Lys40	Lys31
Val41	*Leu41*	*Leu32*
	Arg43	Arg34
Phe44	*Val44*	*Val35*
	Leu45	Leu36
	Gly47	Ser38
Thr75		Thr66
Pro76		Thr67
Tyr77	Tyr77	Asn68
	Pro78	Pro69
Leu79	Leu79	Thr70
Gln80	Leu80	Phe71
	Pro81	Pro72
Ser83	Val83	Cys74
Val84	**Val84**	**Val75**
	Glu86	Asp77
	Val109	Pro100
	Glu111	Glu102
	Asp112	Asp103
Leu113		
Ser114		
	Gln113	Pro104
	Arg114	Arg105
	Leu142	Leu133

The lines in boldface indicate conserved residues in the primary structures of all three PPases. The lines in italics show similar hydrophobic residues among all three PPases. [a]The homology of the primary structures is described in Ref. *11*.

interactions must be important for thermostability. From the three-dimensional structures of both *E. coli* and *Tth.* PPases (*6, 8, 10*), we can predict that the conserved Val75 may locate at the interface between the monomers (Table I). In this study, we tried to examine and confirm the role of Val75 in the oligomeric interactions and thermostability by preparing variants by site-directed mutagenesis in which Val75 is replaced by Ala, Phe, Leu, Ile, Lys, Gln, or Asp.

MATERIALS AND METHODS

Materials and Chemicals—T4 DNA ligation Kit ver. 1 was obtained from Takara Shuzo. Restriction endonucleases were purchased from Nippon Gene and Bio Labs. Gene *Taq* was purchased from Nippon Gene. *Bca* BEST™ dideoxy sequencing kit was purchased from Takara Shuzo. DEAE-Sephacel, Sephacryl S-200HR, and Superdex 75 pg were obtained from Pharmacia. *E. coli*, JM109 strain, was used as a host bacterium for the site-directed mutagenesis and for the expression of recombinant *Bst.* PPase and its variants. The plasmid harboring the *Bst.* PPase gene was constructed as reported previously (*11*).

Preparation of Recombinant Bst. PPase—Recombinant *Bst.* PPase and its variants were purified as reported previously (*11*). Protein concentration was determined by the method of Lowry *et al.* (*15*) using bovine serum albumin as a standard.

Construction of Expression Vectors of Bst. PPase Variants—The replacement of Val75 by Ala, Phe, Leu, Ile, Lys, Gln, and Asp was achieved by exchanging fragments produced by mismach PCR. The mutagenesis primers were 5′-GAC ACG CGT ATC AAT GGC ACA GCC TGG-3′ for substituting Val75 with Ala, 5′-GAC ACG CGT ATC AAT AAA ACA GCC TGG-3′ for substituting with Phe, 5′-GAC ACG CGT ATC AAT TAA ACA GCC TGG-3′ for substituting with Leu, 5′-GAC ACG CGT ATC AAT AAT ACA GCC TGG-3′ for substituting with Ile, 5′-GAC ACG CGT ATC AAT TTT ACA GCC TGG-3′ for Lys, 5′-GAC ACG CGT ATC AAT TTG ACA GCC TGG-3′ for Gln, and 5′-GAC ACG CGT ATC AAT GTC ACA GCC TGG-3′ for Asp. The mutated PCR products for the Val75-Ala, Phe, Leu, Ile, Lys, Gln, and Asp mutations were digested with *Bam*HI-*Mlu*I, and the resulting fragments were inserted into the corresponding position of an original vector, pMK2PPAQ. Mutations in the gene were confirmed by nucleotide sequencing.

DNA Sequencing—DNA sequencing was performed by the dideoxy chain termination method using a *Bca* BEST dideoxy sequencing kit (Takara Shuzo) with a fluorescence DNA sequencer, Hitachi SQ-3000.

Circular Dichroism (CD) Measurements—CD spectra were measured with a JASCO J-600 automatic recording dichrograph at room temperature. Cells with 1 mm pathlengths were used for measurements in the far-ultraviolet region. CD data are expressed as mean residue ellipticity $[\theta]$ using the mean residue molecular weight from the primary structure.

Fluorescence Measurements—Fluorescence measurements were made using a JASCO FP777 spectrofluorometer at room temperature. The protein concentration was always adjusted to 0.05 mg/ml in 20 mM Tris-HCl buffer (pH 7.8). Tryptophan excitation was at 295 nm. The emission spectra were set between 300 and 400 nm.

Assay of Enzyme Activity—PPase activity was assayed at 37°C according to the procedure described previously (*16*) in which the liberation of inorganic phosphate was determined by the method of Peel and Lougman (*17*).

Thermostability—Enzyme preparations were incubated at different temperatures for 1 h in the presence or absence of 1 mM Mg^{2+} at pH 7.8. The remaining activity was measured as described above.

Analysis of Trimer/Monomer State—The molecular weight of recombinant *Bst.* PPase was determined on a HiLoad 26/60 Superdex 75 pg column (Pharmacia) with bed dimensions of 2.6×60 cm. Molecular weight markers were used to determine trimer and monomer. The column was run at room temperature with 50 mM Tris-HCl buffer (pH 7.8) as the eluent (flow rate, 3.0 ml/min). The protein concentration of the applied samples was adjusted to 0.10 mg/ml. Samples were heated at 40, 50, 60, 70, 80, or 90°C for 1 h, then filtered through samprep LCR25-LG (pore size 0.2 mm, Millipore) and injected onto the column. The trimer/monomer ratio was determined by estimating the peak areas from gel filtration with a Shimadzu Chromatopac C-R6A.

RESULTS

Characteristics of the Val75 Variants—As described above, we assumed that Val75 of *Bst.* PPase may contribute to oligomeric interactions on the basis of the three-dimensional structures of *E. coli* and *Tth.* PPases (*6, 8, 10*) and homology of the primary structure between *Bst.* PPase and the other two PPases (Table I). Therefore, we constructed seven Val75-substituted variants (V75A, V75F, V75L, V75I, V75K, V75Q, and V75D) to evaluate the contributions of Val75 to the thermostability and oligomeric interactions.

First, the specific activities of the valine-replaced variants, V75A, V75F, V75L, V75I, V75K, V75Q, and V75D, were measured (Table II). V75A, V75F, V75L, and V75I showed more than 75% of the activity of the wild type, but V75Q showed less than 40%, and V75D and V75K showed less than 30 and 10%, respectively (Table II). These results indicate that the variants in which valine is replaced by hydrophobic residues still retains considerable enzyme activity, whereas variants with hydrophilic residue substitutions show drastically decreased activity, especially in the case of charged polar side chains. Thus, the hydrophobic environment around Val75 is critical to maintaining enzyme activity and a hydrophilic environment produces a prominent reduction in activity, especially if the substitute contains a negative or positive charge. To examine the conformational changes caused by the substitutions, the conformations of the variants were investigated by measuring the CD spectra in the far-UV region. The CD spectra showed the presence of secondary structures such as α-helix and β-sheet, and the substituted variants showed almost the same CD spectra as the wild type (Fig. 1). From these results, we can conclude that these mutations do not influence the secondary structure of the molecule.

Thermostability of Enzyme Activity—In order to characterize the thermostability of *Bst.* PPase and its variants, the enzymes were incubated at various temperatures (40–90°C) for 1 h, and the remaining activity was measured after cooling. V75A, V75F, V75L, and V75I showed almost the same inactivation behavior as the wild type enzyme, with a melting temperature of about 60°C (Fig. 2a). On the other hand, the activities of V75K, V75Q, and V75D decreased more rapidly than the wild type, with melting

TABLE II. **The enzyme activity of recombinant *Bst.* PPase and its Val75-substituted variants.**

Substituted variant	Enzyme activity	
	Specific activity (units/mg)	Relative activity[a] (%)
Wild type	687	100
V75A	673	98.0
V75I	602	87.6
V75F	523	76.1
V75L	580	84.4
V75Q	254	37.0
V75D	195	28.4
V75K	59	8.59

[a]The specific activity of recombinant *Bst.* PPase (wild type) was taken as 100%.

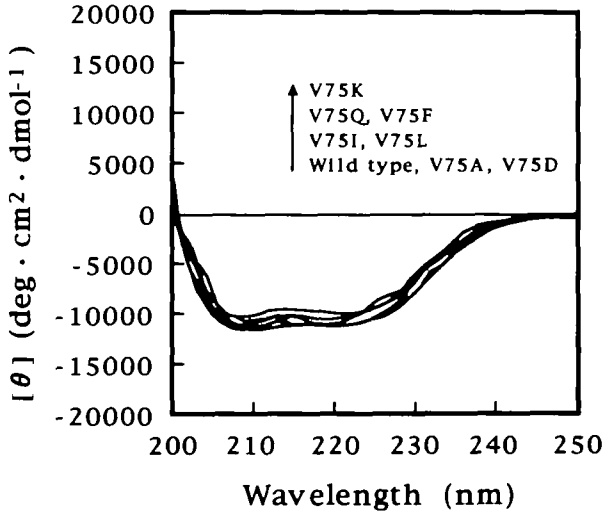

Fig. 1. **Far-UV CD spectra of *Bst.* PPase (wild type) and Val75-replaced variants.** The CD spectra were measured under the conditions described in "MATERIALS AND METHODS."

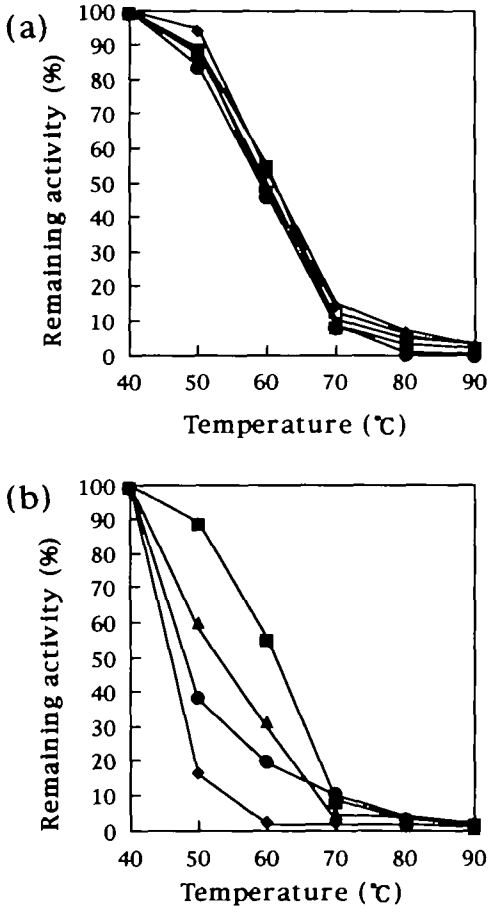

Fig. 2. **Thermostability of *Bst.* PPase (wild type) and Val75-replaced variants.** The enzyme (0.1 mg/ml) was incubated in Tris-HCl buffer (pH 7.8) at various temperatures for 1 h. Then the enzyme activity was measured at 37°C after rapid cooling, and the activity at 40°C was taken as 100%. (a) ■, wild type; ●, V75A; ▲, V75F; ◆, V75L; □, V75I; (b) ■, wild type; ●, V75K; ▲, V75Q; ◆, V75D.

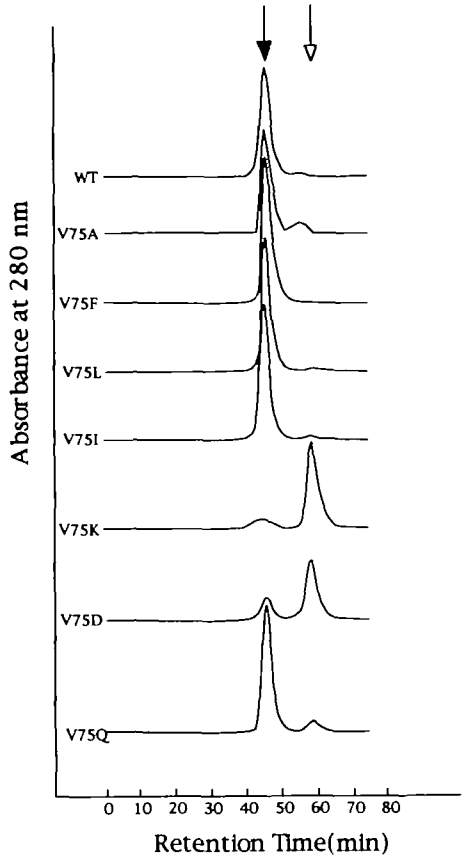

Fig. 3. **The elution profiles of FPLC for *Bst.* PPase (wild type) and Val75-replaced variants.** The black and white arrows indicate the retention times for the trimer and monomers, respectively. A Superdex 75 pg column was used, and the flow rate was 3 ml/min, eluted with 50 mM Tris-HCl (pH 7.8).

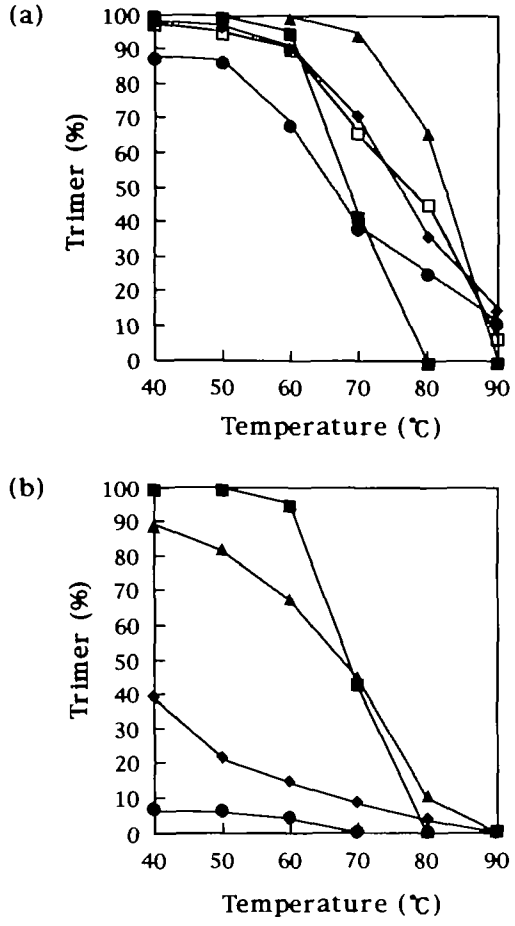

Fig. 4. **Dissociation of trimeric *Bst.* PPase (wild type) and Val75-replaced variants into monomers by heat treatment.** The enzyme (0.1 mg/ml) was incubated in Tris-HCl buffer (pH 7.8) at various temperatures for 1 h. A Superdex 75 pg column was eluted at a flow rate of 3 ml/min with 50 mM Tris-HCl (pH 7.8). The dissociation ratio was estimated from the peak area of trimer plus that of the monomer in the FPLC elution profiles and taken as 100%. (a) ■, wild type; ●, V75A; ▲, V75F; ◆, V75L; □, V75I; (b) ■, wild type; ●, V75K; ▲, V75Q; ◆, V75D.

temperatures of about 50°C, 55°C, and 47°C, respectively (Fig. 2b). These results indicate that variants with hydrophobic residue replacements have almost the same thermostability as the wild type enzyme, while variants with hydrophilic residue replacements are evidently less thermostable. Therefore, we can conclude that the presence of a hydrophobic residue at this location is crucial for thermostability.

Assay of Dissociation into Subunits by Heat Treatment—Oligomeric interactions are sometimes very important to the thermostability of a protein, and there are many cases in which the amino acid residues located at the interface between the subunits may play a key role in the oligomeric interactions. First, we evaluated the quaternary structure of Val75 variants in the native state. As a result, the wild type, V75F, V75L, and V75I were found to show no dissociation in the native state, while V75A and V75Q were slightly dissociated. However, V75K and V75D showed greater than 70% dissociation without heating (Fig. 3). The molecular weights of the first and second peak from gel filtration correspond to the trimer and monomer, respectively. We observed a subpeak (retention time 55 min) on the profile of the wild type and V75A that seems to correspond to the dimer, but we can not confirm this component. Next, the dissociation assay of trimeric *Bst.* PPase by heat treatment was carried. We estimated the trimer/monomer ratios for the wild type enzyme and all valine-replaced variants upon heating at various temperatures. The half point (trimer:monomer = 1:1) for the wild type was found to be 68°C, V75A and V75Q were 66°C, and V75F, V75L, and V75I were 83, 75, and 78°C, respectively (Fig. 4, a and b). We could not estimate the half points for V75K and V75D, because they were already more than 50% dissociated in the native state (Fig. 4b). The results indicate that variants in which valine is replaced by Ala and Gln show similar dissociation behavior as the wild type, while variants with Phe, Leu, and Ile substitutions are rather stable to heat dissociation. However, variants with Asp and Lys substitutions dissociate to monomers even at room temperature, indicating considerable lability of the molecule.

DISCUSSION

In general, thermophilic enzymes are more thermostable than mesophilic enzymes, and the factors contributing to

their thermostability have been deduced for some enzymes (*18, 19*). In the case of PPases, many thermophilic PPases are more thermostable than mesophilic PPases, such as *E. coli* and Y-PPases (*16, 20, 21*). However, the reason for this thermostabilization is little understood. A common characteristic of PPases is that they form oligomeric structures such as dimers, trimers, and hexamers. Therefore, we predicted that a clue to understanding the thermostabilization of thermophilic PPases may lie in the oligomeric interactions of each PPase.

As described above, the three-dimensional structures of *Tth.* and *E. coli* PPases have been determined at 2.0 and 1.9 Å resolution, respectively (*6, 8, 10*). From a comparison of the three-dimensional structures, it was hypothesized that the thermostabilization of *Tth.* PPase may be due to the difference in the oligomeric interactions (*10*). On this basis, we investigated the residues contributing to the oligomeric interactions in *Bst.* PPase. From the homology between the primary structures of *Bst.*, *E. coli*, and *Tth.* PPases (Table I), we focused on Val75 in *Bst.* PPase, which corresponds to Val84 in both *E. coli* and *Tth.* PPases (*11*), and constructed seven Val75-substituted variants.

In this study, we suggest that the hydrophobicity of Val75 in *Bst.* PPase may contribute to the oligomeric interactions. We assumed that the main reason for the increase in the oligomeric interaction of V75F, V75L, and V75I may be the bulkiness of the side chain of the substituted amino acid. The average volume of Phe, Leu, and Ile are 203.4, 167.9, and 168.8 Å^3, respectively, while that of Val is 141.7 Å^3 (*22*). Thus, the interacting distances in these variants are significantly closer than that of the wild type (Val), and so they can interact more strongly. When charged amino acids such as Lys and Asp are introduced, some repulsive force occurs, and the interactions are appreciably reduced. There seems to be no significant effect of Ala and Gln substitutions with respect to heat treatment, but these variants are slightly dissociated even in the native state (Fig. 3). Thus, the replacement of Val75 by Ala, with a relatively small side chain, or Gln, with a hydrophilic side chain, produces no essential effect on the oligomeric interactions.

Meanwhile, the CD spectra in the far UV region showed no remarkable differences between the wild type enzyme or any of the variants after heat treatment (data not shown). Therefore, the heat denaturation of the secondary structures of the wild type enzyme and its variants show the same tendency. This suggests that the different inactivations occur because of the differences in the dissociation of the intact molecule into subunits. From these results, we can predict that a hydrophobic residue located in the Val75 region may be critical for the oligomeric interactions, and its hydrophobic interactions with the surroundings may play a key role in thermostability.

As shown in Fig. 5, a and b, the residues in the vicinity of the corresponding Val84 in *E. coli* and *Tth.* PPases were determined from the three-dimensional structure (*6, 8, 10*). Salminen *et al.* reported that Val84 in *E. coli* PPase forms intratrimeric interactions with Leu39 and Val41, while Val84 in *Tth.* PPase forms such interactions with Ile39 and Leu41 (*10*). Although these interactions are formed by the main-chain, we deduce that the region around these residues is located in a hydrophobic environment. In *Bst.* PPase, the corresponding residues are presumed to be Val75, Phe30, and Leu32. All these residues are conserved in the primary structure in terms of being hydrophobic residues. Similar interactions around Val75 may be crucial for maintaining the trimeric subunit structure of *Bst.* PPase.

It has been reported that His136- and His140-replaced variants of *E. coli* PPase dissociate from the hexamer into trimers and show decreased affinities for Mg_2PP_i and Mg^{2+}; therefore, these histidine residues are assumed to be key residues in the trimer-trimer interface, and that hexamer formation improves the substrate binding characteristics

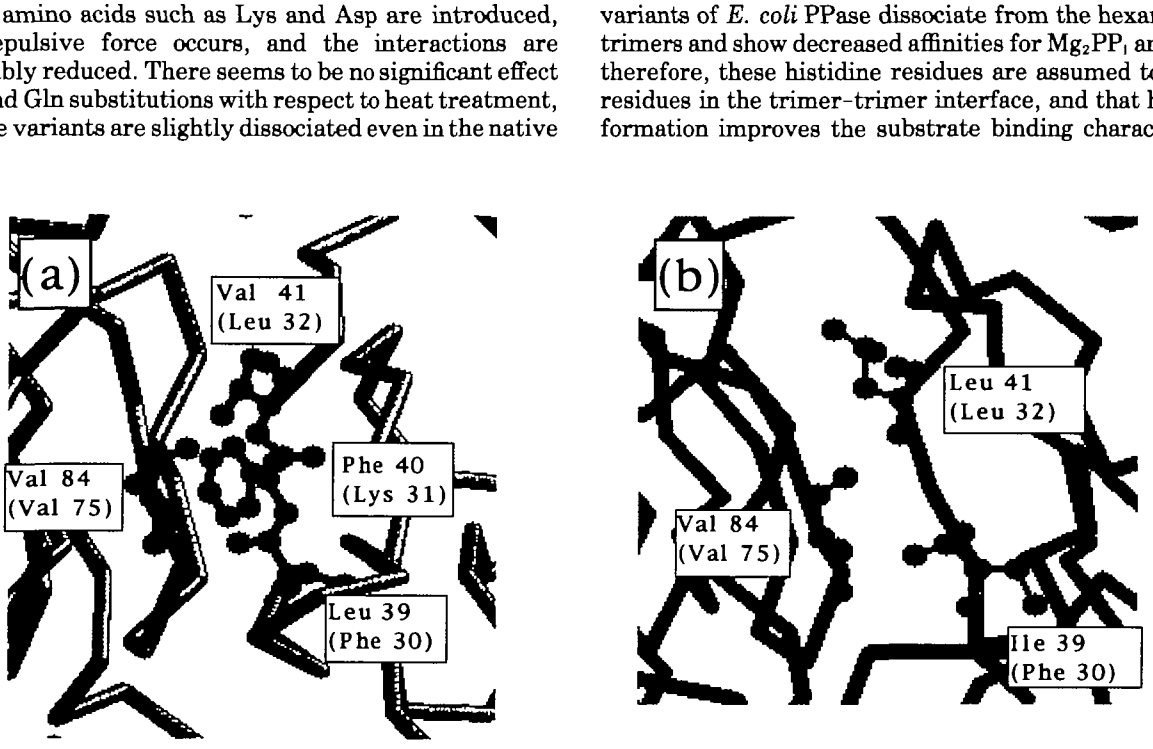

Fig. 5. **Three-dimensional structures of *E. coli* (a) and *Tth.* (b) PPases in the vicinity of the intermonomeric interface.** The three-dimensional structures of *E. coli* PPase (*6*) and *Tth.* PPase (*8*) were drawn by a Molecular Graphics Program, RasMol ver. 2.6. The X-ray structural data for *E. coli* PPase were obtained from the protein Data Bank (PDB code 1obw). That of hexameric *Tth.* PPase was kindly provided by Dr. Teplyakov. The ball and stick representations indicate the side chain of each residue. The residues and numbers in parentheses indicate the corresponding positions in *Bst.* PPase.

(*7, 23*). This dissociation from hexamer to trimers is also observed with substitutions of Glu20, Tyr55, and Lys104 to Asp, Phe, and Arg, respectively, all located within the active site cavity of *E. coli* PPase (*24, 25*). However, *Bst.* PPase exists normally as a trimer and His125 (corresponding to His136 in *E. coli* PPase) is conserved, whereas there is no histidine residue corresponding to His140 in *E. coli* PPase. From these facts, the mechanism of hexamer formation for the substrate binding of *E. coli* PPase may be different from that of *Bst.* PPase. The thermostabilization of *Bst.* PPase must depend on the maintenance of monomer–monomer interactions. Therefore, we conclude that trimer formation by Val75 in *Bst.* PPase may play an important role in thermostability.

REFERENCES

1. Lahti, R. (1983) Microbial inorganic pyrophosphatases. *Microbiol. Rev.* **47**, 169-179
2. Hachimori, A., Shiroya, Y., Hirato, A., Miyahara, T., and Samejima, T. (1979) Effects of divalent cations on thermophilic inorganic pyrophosphatase. *J. Biochem.* **86**, 121-130
3. Heikinheimo, P., Pohjanjoki, P., Helminen, A., Tasanen, M., Cooperman, B.S., Golderman, A., Baykov, A., and Lahti, R. (1996) A site-directed mutagenesis study of *Saccharomyces cerevisiae* pyrophosphatase. Functional conservation of the active site of soluble inorganic pyrophosphatases. *Eur. J. Biochem.* **239**, 138-143
4. Heikinheimo, P., Lehtonen, J., Baykov, A., Lahti, R., Cooperman, B.S., and Golderman, A. (1996) The structural basis for pyrophosphatase catalysis. *Structure* **4**, 1491-1508
5. Pohjanjoki, P., Lahti, R., Goldman, A., and Cooperman, B.S. (1998) Evolutionary conservation of enzymatic catalysis: quantitative comparison of the effects of mutation of aligned residues in *Saccharomyces cerevisiae* and *Escherichia coli* inorganic pyrophosphatase on enzymatic activity. *Biochemistry* **37**, 1754-1761
6. Harutyunyan, E.H., Oganessyan, V.Y., Oganessyan, N.N., Avaeva, S.M., Nazarova, T.I., Vorobyeva, N.N., Kurilova, S.A., Huber, R., and Mather, T. (1997) Crystal structure of holo inorganic pyrophosphatase from *Escherichia coli* at 1.9 Å resolution. Mechanism of hydrolysis. *Biochemistry* **36**, 7754-7760
7. Baykov, A.A., Dudarenkov, V.Y., Käpylä, J., Salminen, T., Hyytiä, T., Kasho, V.N., Husgafvel, S., Cooperman, B.S., Goldman, A., and Lahti, R. (1995) Dissociation of hexameric *Escherichia coli* inorganic pyrophosphatase into trimers on His-136→Gln or His-140→Gln substitution and its effect on enzyme catalytic properties. *J. Biol. Chem.* **270**, 30804-30812
8. Teplyakov, A., Obmolova, G., Wilson, K.S., Ishii, K., Kaji, H., Samejima, T., and Kuranova, I. (1994) Crystal structure of inorganic pyrophosphatase from *Thermus thermophilus*. *Protein Sci.* **3**, 1098-1107
9. Satoh, T., Samejima, T., Watanabe, M., Nogi, S., Takahashi, Y., Kaji, H., Teplyakov, A., Obmolova, G., Kuranova, I., and Ishii, K. (1998) Molecular cloning, expression and site-directed mutagenesis of inorganic pyrophosphatase from *Thermus thermophilus* HB8. *J. Biochem.* **124**, 79-88
10. Salminen, T., Teplyakov, A., Kankare, J., Cooperman, B.S., Lahti, R., and Goldman, A. (1996) An unusual route to thermostability disclosed by the comparison of *Thermus thermophilus* and *Escherichia coli* inorganic pyrophosphatases. *Protein Sci.* **5**, 1014-1025
11. Satoh, T., Shinoda, H., Ishii, K., Koyama, K., Sakurai, N., Kaji, H., Hachimori, A., Irie, M., and Samejima, T. (1999) Primary structure, expression and site-directed mutagenesis of inorganic pyrophosphatase from *Bacillus stearothermophilus*. *J. Biochem.* **125**, 48-57
12. Maruyama, S., Maeshima, M., Nishimura, M., Aoki, M., Ichiba, T., Sekiguchi, J., and Hachimori, A. (1996) Cloning and expression of the inorganic pyrophosphatase gene from thermophilic bacterium PS-3. *Biochem. Mol. Biol. Int.* **40**, 679-688
13. Schreier, E. and Höhne, W.E. (1978) Kinetic characterization of inorganic pyrophosphatase from *Bacillus stearothermophilus*. *FEBS Lett.* **90**, 93-96
14. Schreier, E. (1980) Reversible acid dissociation of thermostable inorganic pyrophosphatase from *Bacillus stearothermophilus*. *FEBS Lett.* **109**, 67-70
15. Lowry, O.H., Rosebrough, N.J., Farr, A.L., and Randall, R.J. (1951) Protein measurement with the Folin phenol reagent. *J. Mol. Chem.* **193**, 265-275
16. Hachimori, A., Takeda, A., Kaibuchi, M., Ohkawara, N., and Samejima, T. (1975) Purification and characterization of inorganic pyrophosphatase from *Bacillus stearothermophilus*. *J. Biochem.* **77**, 1177-1183
17. Peel, J.L. and Loughman, B.C. (1957) Some observations on the role of copper ions in the reduction of phosphomolybdate by ascorbic acid and their application in the determination of inorganic orthophosphate. *Biochem. J.* **65**, 709-716
18. Moriyama, H., Onodera, K., Sakurai, M., Tanaka, N., Kirino, H.K., Oshima, T., and Katsube, Y. (1995) The crystal structures of mutated 3-isopropylmalate dehydrogenase from *Thermus thermophilus* HB8 and their relationship to the thermostability of the enzyme. *J. Biochem.* **117**, 408-413
19. Veltman, O.R., Vriend, G., Hardy, F., Mansfeld, J., Van den burg, B., Venema, G., and Eijsink, V.G. (1997) Mutational analysis of a surface area that is critical for the thermal stability of thermolysin-like proteases. *Eur. J. Biochem.* **248**, 433-440
20. Meyer, W., Moll, R., Kath, T., and Schäfer, G. (1995) Purification, cloning, and sequencing of archaebacterial pyrophosphatase from the extreme thermoacidophile *Sulfolobus acidocaldarius*. *Arch. Biochem. Biophys.* **319**, 149-156
21. Richter, O.M.H. and Schäfer, G. (1992) Purification and enzymic characterization of the cytoplasmic pyrophosphatase from the thermoacidophilic archaebacterium *Thermoplasma acidophilum*. *Eur. J. Biochem.* **209**, 343-349
22. Chothia, C. (1975) Structural invariants in protein folding. *Nature* **254**, 304-308
23. Velichko, I.S., Mikalahti, K., Kasho, V.N., Dudarenkov, V.Y., Hyytiä, T., Goldman, A., Cooperman, B.S., Lahti, R., and Baykov, A.A. (1998) Trimeric inorganic pyrophosphatase of *Escherichia coli* obtained by directed mutagenesis. *Biochemistry* **37**, 734-740
24. Volk, S.E., Dudarenkov, V.Y., Käpylä, J., Kasho, V.N., Voloshima, O.A., Salminen, T., Goldman, A., Lahti, R., Baykov, A.A., and Cooperman, B.S. (1996) Effect of E20D substitution in the active site of *Escherichia coli* inorganic pyrophosphatase on its quaternary structure and catalytic properties. *Biochemistry* **35**, 4662-4669
25. Fabrichniy, I.P., Kasho, V.N., Hyytiä, T., Salminen, T., Halonen, P., Dudarenkov, V.Y., Heikinheimo, P., Chernyak, V.Y., Goldman, A., Lahti, R., Cooperman, B.S., and Baykov, A.A. (1997) Structural and functional consequences of substitutions at the tyrosine 55-lysine 104 hydrogen bond in *Escherichia coli* inorganic pyrophosphatase. *Biochemistry* **36**, 7746-7753